J. Materials, Conc. Struct., Pavements No. 532/V-30, 221-233, February 1996

A FRACTURE MECHANICS-BASED DESIGN METHOD FOR SFRC TUNNEL LININGS

Pruettha NANAKORN[1], Hideyuki HORII[2] and Shigeru MATSUOKA[3]

[1]Member of JSCE, D.Eng., Assistant Professor, Dept. of Civil Eng., The University of Tokyo (Bunkyo-Ku, Tokyo 113, Japan)

[2]Member of JSCE, Ph.D., Associate Professor, Dept. of Civil Eng., The University of Tokyo (Bunkyo-Ku, Tokyo 113, Japan)

[3]Member of JSCE, B.Eng., Chief Research Engineer, Institute of Technology, Tekken Corporation (Chiyoda-Ku, Tokyo 101, Japan)

The recently established Japanese design provision on the estimation of the load-carrying capacity of steel-fiber-reinforced concrete (SFRC) tunnel linings is based on the concept of fracture mechanics of concrete. Existence of a crack and stress transmission by fibers are considered in the estimation of the maximum resultant forces of the critical cross-section. In this study, the validity of the current design method is verified, and the possible improvements of the design method are proposed.

Key Words: *tunnel lining, design, steel-fiber-reinforced concrete, fracture mechanics, tension-softening relationship*

1. INTRODUCTION

The fracture mechanics of concrete has been extensively studied during the past decade. The objectives of the studies have been to understand the behavior of concrete under application of loads and to be able to predict the fracture behavior of concrete under general boundary conditions and loadings. Until now, the governing mechanisms have already been captured, especially for mode one crack growth phenomena. General agreement on governing mechanisms, their modeling, material characterization and analysis methods has been attained to some extent. The studies on the fracture mechanics of concrete have now moved from the initial and pioneering period to the second stage. Tasks in the second stage of the studies on the fracture mechanics of concrete include:

(a) establishment of analysis tools for the general behavior of concrete structures including tensile and compressive fracture phenomena,

(b) application of fracture mechanics to design practice, and

(c) development and design of new materials based on the fracture mechanics and micromechanics of cementitious composites.

Recently, a new design provision for steel-fiber-reinforced concrete (SFRC) tunnel linings was completed in Japan[1]. The design provision is based on the concept of the fracture mechanics of concrete. To estimate the load carrying capacity of the critical cross-section, existence of a crack and transmission of stress by fibers are considered. In the present paper, the fracture mechanics of concrete is first reviewed in brief. Then the current fracture mechanics-based design provision is concisely introduced, and its points to be improved are shown. Finally, a proposal of a modified design method, which can be used to estimate the load-carrying capacities of tunnel linings with various thickness and different kinds and volume fractions of fibers, is presented.

2. FRACTURE MECHANICS OF CONCRETE

It is well accepted that the Linear Elastic Fracture Mechanics (LEFM) approach cannot directly be applied to concrete because of the existence of a large fracture process zone near the crack tip. The fracture process zone can be categorized into two

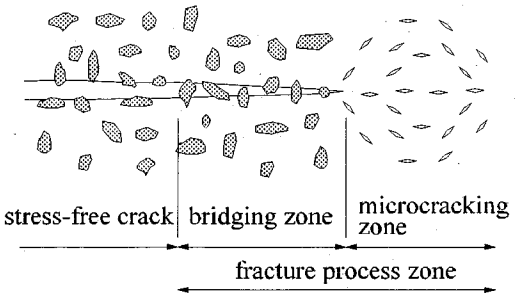

Fig.1 Schematic illustration of fracture process zone.

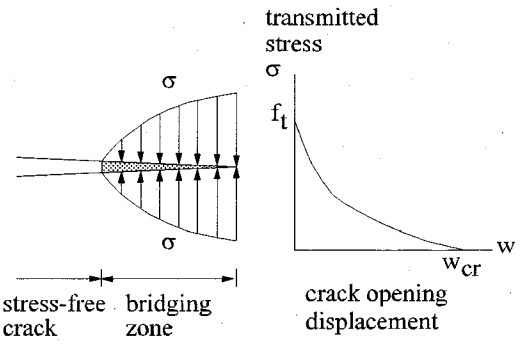

Fig.2 Dugdale-Barenblatt type model with a tension-softening relationship.

zones with different dominant mechanisms, namely microcracking zone and bridging zone (see **Fig.1**). The microcracking zone is a zone where the initiation of microcracks and their growth are dominant. Microcracking is sometimes understood as an ensemble of microevents such as the extension of existing defects and pores, and the debonding at the interfaces between aggregates and the cement matrix rather than the actual cracking. The bridging zone is a part of macrocrack along which the stress is transmitted by aggregates and fibers.

Many models have been proposed to predict the crack growth behavior of concrete. In the field of fracture mechanics, a model for the nonlinear zone ahead of the crack in metallic materials was proposed by Dugdale[2]. In his model, the nonlinear zone is modeled as an extension of the actual crack and perfectly plastic behavior is assumed along this crack extension. In a slightly different way, Barenblatt[3] considered molecular forces of cohesion acting on the edge region of the crack. Barenblatt limited the analysis to cases where the size of the edge region with cohesion is small compared to the size of the whole crack. The idea of Dugdale and Barenblatt have been extended to the fracture of disordered materials such as concrete, rock and ceramics. Hillerborg et al.[4] proposed the Fictitious Crack Model (FCM) in which the fictitious crack ahead of the actual crack is assumed, and the crack closure stress along this fictitious crack is considered. In the model, the crack is assumed to propagate when the stress at the crack tip reaches the tensile strength. When the crack opens, the stress is assumed to decrease with increasing crack opening displacement. The crack closure stress can be determined from a tension-softening relationship corresponding to the post-peak stress-displacement relationship of the uniaxial tension test.

Unlike the fictitious crack model or the Dugdale-Barenblatt type model, both of which consider the whole nonlinear zone as only an extension of the actual crack with the transmitted stress, the model proposed by Nirmalendra and Horii[5] considers the effects from microcracking and bridging separately. The two mechanisms are separately modeled, the Dugdale-Barenblatt type model being used to model bridging alone. In this model, bridging obeys the tension-softening curve while microcracking obeys a microcracking law. The model is applied to concrete, and the result shows that the effect of microcracking on the toughness of concrete is small, and bridging is the governing mechanism of the crack growth in concrete.

In this study, the attention will be paid only to bridging in the modeling of the fracture process zone; even if microcracking exists, its effects are negligible. It is then straightforward to adopt the Dugdale-Barenblatt type model with a tension-softening curve (see **Fig.2**) to model the fracture behavior of concrete.

3. FRACTURE MECHANICS-BASED DESIGN PROVISION FOR SFRC TUNNEL LININGS

Recently the Extruded Concrete Lining (ECL) has been introduced in Japan in order to improve the quality of construction, economic efficiency and working conditions and to save labor. In this method, excavation and lining placement are carried out in parallel, and the concrete lining is constructed in close contact with the surrounding ground. In ECL, the concrete lining contains no steel-bar reinforcement, and plain concrete is usually used. However, since the past few years, the steel-fiber-reinforced concrete has become a competitive choice

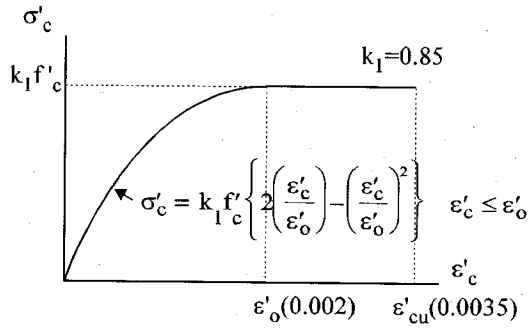

Fig.3 Design uniaxial compressive stress-strain curve.

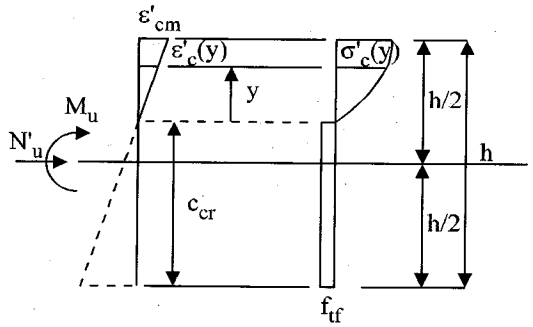

$c_{cr} \leqq 0.7h$ for the current provision.

Fig.4 Design stress distribution for the estimation of sectional force capacity.

because of its higher tensile resistance and remarkable toughness. The cross-sections of linings are expected to be smaller if the steel-fiber-reinforced concrete is used in place of plain concrete.

In the design of concrete tunnel linings, one of the limit states is the failure of a section after initiation and propagation of a crack. An increase in maximum resultant forces and greater toughness after the peak load are expected in linings with SFRC, due to the stress transmission across crack surfaces by fibers. To reflect such benefits of steel fibers in design, the design provision must take this stress transmission into account. This implies that a new design method is required since the conventional method ignores resistance to tensile stress. Knowledge of fracture mechanics is applied since the limit state is governed by the growth of a crack and the stress transmission across it.

In 1992, "Recommendation for Design and Construction of Extruded Concrete Lining Method" was completed by Japan Railway Construction Public Corporation[1]. This is a design provision that is based on fracture mechanics. The main assumptions in the evaluation of the sectional capacity are as follows:

(a) axial strain in compression is proportional to the distance from the neutral axis,

(b) stress-strain curve in compression for SFRC members follows that shown in **Fig.3**,

(c) tensile strength carried by fibers, f_{tf}, is considered for the tensile stress in SFRC members, and

(d) the maximum length of the crack is 70% of the thickness of the lining.

Fig.4 shows the stress distribution used in the evaluation of the sectional capacity in the design provision. The design method is based on the results of experiments. Even though the basic idea of fracture mechanics is employed through the introduction of the stress transmission along a crack, some assumptions are introduced, more or less, without clear supporting background. One of the points to be clarified is the validity of the assumption of the stress distribution. In the current design provision, the tensile strength carried by fibers f_{tf} is constantly assumed along the crack. In reality, the transmitted tensile stress decreases with increasing crack opening displacement in a way that agrees with the tension-softening relationship. Another important point to be investigated is the assumption of the maximum crack length. In the current design provision, the maximum crack length equal to 70% of the thickness of the lining is assumed. Since the estimated bending moment capacity is larger with longer crack length, an improper selection of the critical crack length will lead to either too conservative or unsafe design.

In the current design provision, it is specified that the tensile strength carried by fibers f_{tf} is to be determined from a bending test. However, if the same crack length is employed in the determination of f_{tf} from a small bending specimen, the obtained fiber stress f_{tf} overestimates the bending moment capacities of linings with larger thickness. The limitation of the crack length results in safe design for the estimation of load-carrying capacity while the limitation of the crack length in the evaluation of the tensile strength carried by fibers leads to less safe design. Although, in the current design provision, a factor for the member size is introduced, the magnitude of the factor is determined without theoretical support. Consequently, it is desirable to identify the source of the size effect and to develop a design method without unclear factors.

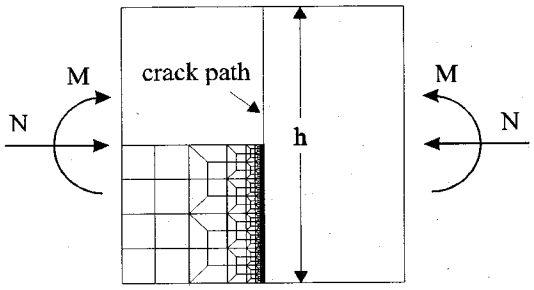

Fig.5 Numerical analysis of the critical section.

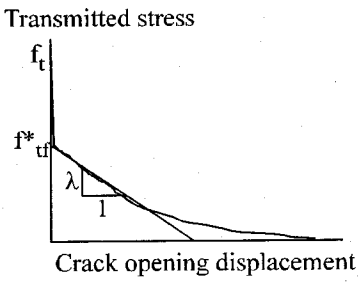

Fig.6 Tension-softening curve and linear approximation.

4. CRACK GROWTH ANALYSIS OF THE CRITICAL SECTION

(1) Numerical analysis of the critical section

Instead of carrying out experiments and measurements at the critical section of SFRC tunnel linings, we solve the problem shown in **Fig.5** by FEM analysis. It is a plane strain problem under the applied bending moment and axial compressive force. The unit thickness of the specimen is considered for all calculations. Horii and Nanakorn[6] showed that consideration of a single crack at the critical section is sufficient even if there are distributed cracks at the initial stage. Therefore, only a single crack at the middle of the specimen is considered in the calculations. The mesh used in the calculations is refined in such a way that a fine mesh is obtained along the crack path as shown in **Fig.5**. Note that, in the mesh, there are 256 elements along the crack path. The complete mesh topology can be obtained from **Fig.5** by considering the symmetry.

The propagation of the crack is captured by a cracked element which is an element with embedded displacement discontinuity[7]. In the element, the stress-displacement jump relationship, which is the tension-softening relationship, is satisfied at the discontinuity surface. The tension-softening relationship can be obtained from the post-peak stress-displacement relationship of the direct tension test. However, the direct tension test is difficult to perform because the behavior after the peak is unstable unless a very stiff machine is used. To avoid this difficulty, Nanakorn and Horii[8] proposed a back analysis method to obtain the tension-softening relationship from a bending test of a notched beam.

It is observed from experimental results that the tension-softening curve of SFRC usually exhibits a sharp-drop part at the beginning of the curve, which can be neglected for the practical consideration of the design method[9]. After the sharp drop, the tension-softening curve has a gentle slope (see **Fig.6**). Therefore, it can be reasonably represented by a linear tension-softening relationship as shown in **Fig.6**. Note that f^*_{tf} represents the stress after the sharp drop in the real tension-softening curve, and the slope of the linear tension-softening curve is denoted by λ. For the nonlinear behavior in compression, a Drucker-Prager type constitutive equation with the same uniaxial stress-strain curve as the existing design provision is employed (see **Fig.3**).

The height of the sample considered in the computations is equal to the thickness of the lining. The length of the sample should be long enough to enclose the zone disturbed by the failure surface. Horii and Nanakorn[6] showed that the length of the square sample is sufficient. Thus, square specimens are used in all analyses.

(2) Stress distributions in samples with different sizes

At first, the size effect in SFRC linings is investigated. In the design of tunnel linings, the better understanding in the effect of size to the behavior of linings is very important. This is because the capacity of the design section will be estimated from the results of experiments which are normally conducted on relatively small specimens. Therefore, if the size effect is not well understood, the sensible prediction can not be expected. For the investigation, samples with heights of 150 mm, 200 mm, 300 mm and 400 mm, are analyzed with only the applied bending moment using FEM. Material properties used in the computations are shown in **Fig.7**. In the same figure, the axial stress distributions, obtained from the analyses, along the critical cross-section at peak loads for all problems are plotted with distance along the cross-section normalized by the lining thickness. Only the transmitted tensile stress distribution along the tensile stress region is enlarged and shown in **Fig.8**. It is noticed that the transmitted

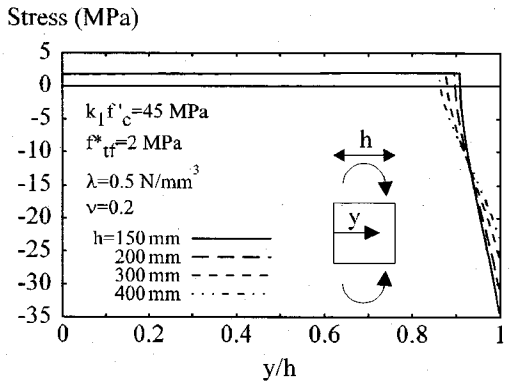

Fig.7 Stress distributions along the critical section of samples with different sizes.

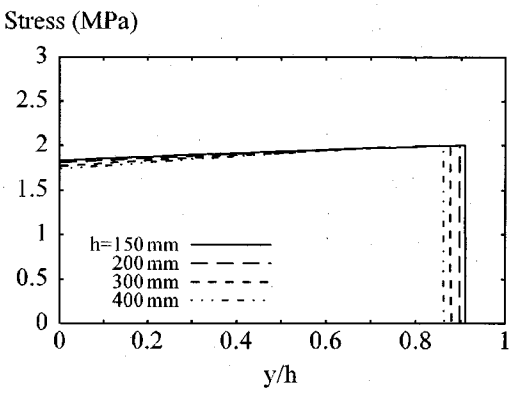

Fig.8 Transmitted tensile stress distributions along the critical section of samples with different sizes.

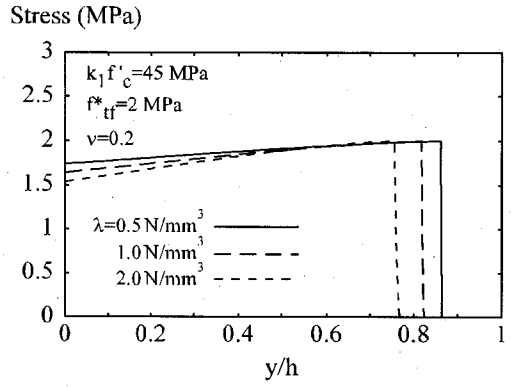

Fig.9 Stress distributions along the critical section with tension-softening curves with different slopes.

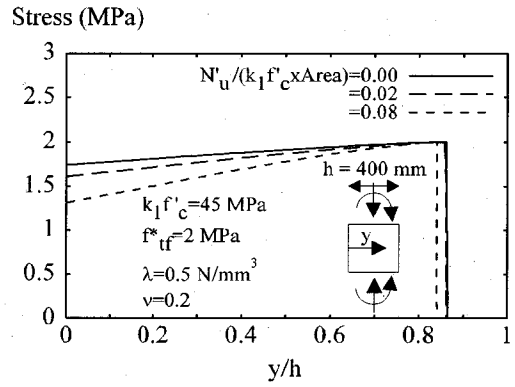

Fig.10 Stress distributions of samples with different axial compressive forces.

tensile stresses in all cases look almost the same and are almost constant along their cracks. The crack lengths at the peak loads, on the other hand, are different. The difference is expected to be greater when bridging by fibers is weaker and the material behavior is closer to that of plain concrete.

(3) Stress distributions in samples with different slopes of tension-softening curves

The tension-softening curve is known to be one of the material properties that control the fracture behavior of concrete. Here, the effect of the slope of the tension-softening curve on the stress distribution at the peak load is investigated. The slope of the linear tension-softening curve is varied inside the reasonable range for SFRC. The problems are analyzed with only applied bending moment. The obtained transmitted tensile stress distributions along the tensile stress region at the peak loads are plotted in **Fig.9**. It is expected that the reduction of the transmitted stress is greater when the slope of the tension-softening curve is steeper. In plain concrete, it is possible to have a stress-free crack at the peak load. This means that there is no transmitted stress along some parts of the crack. However, in SFRC with λ less then 2 N/mm^3, such a great reduction in the transmitted stress is not observed in the pure bending case as seen in **Fig.9**. It is also observed from the figure that the crack length at the peak load decreases with the steeper slope of the tension-softening curve.

(4) Stress distributions in samples with the axial compressive force

Next, we consider the problem with the application of the axial compressive force and bending moment. Here, the section with the height of 400 mm is analyzed with different applied axial compressive forces. **Fig.10** shows the obtained transmitted tensile stress distributions along the tensile stress region at the maximum bending moments. It is seen that the transmitted tensile stress distribution changes when

there is the applied axial compressive force. With the application of the axial compressive force, the crack opening displacement at the peak load becomes larger, and accordingly the transmitted tensile stress becomes smaller as it follows the tension-softening relationship. This effect is greater when the magnitude of the applied axial compressive force is larger. It is noticed that the crack length at the peak load tends to decrease with increasing axial compressive force.

5. PROPOSAL OF A DESIGN METHOD

(1) Estimation of the sectional capacity

Judging from the results of the previous section, we find that it is reasonable to adopt the assumption of the constant tensile stress along the crack; this is the assumption employed in the current design recommendation. However, it is also noticed that, when the applied axial compressive force is large, the tensile stress distribution can be different from the constant one. Therefore, a method to take care of this point will be included in the following proposed design method, and it will be discussed afterwards.

First, let us consider a design stress distribution shown in **Fig.4**. The sectional forces can be written as

$$N'/b = \int_0^{h-c} \sigma'_c(y)dy - \sigma_{tf}c \quad , \tag{1}$$

$$M/b = \int_0^{h-c} \sigma'_c(y)\left(y + c - \frac{h}{2}\right)dy + \sigma_{tf}c\left(\frac{h}{2} - \frac{c}{2}\right) \tag{2}$$

where b is the width of the sample and σ_{tf} is the tensile stress carried by fibers which is the assumed constant transmitted tensile stress along the crack at any loading state. Note that the tensile stress carried by fibers σ_{tf} used in the evaluation of the sectional force capacities M_u and N'_u is called the tensile strength carried by fibers and is denoted by f_{tf}.

Employing the assumption that the axial strain beyond the cracking region is proportional to the distance from the neutral axis, we write

$$\varepsilon'_c = \frac{\varepsilon'_{cm}}{h-c}y \tag{3}$$

where ε'_{cm} is the compressive strain at the top of the section.

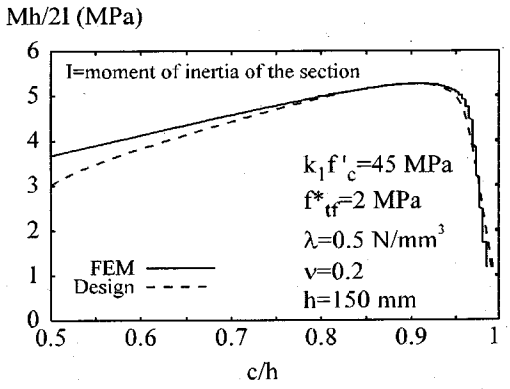

Fig.11 Crack length from the design method.

From Eqs.(1), (2) and (3) and given values of ε'_{cm}, N′ and M, one can calculate the tensile stress carried by fibers σ_{tf} and the crack length c. Or equivalently M is calculated for given values of N′, σ_{tf} and c. To show the validity of this estimation method, the following numerical investigation is performed. For N′ = 0, FEM analysis is carried out. The relationship between the applied moment M and the crack length c is obtained, and the result is plotted in **Fig.11**. Then Eqs.(1), (2) and (3) are employed to calculate σ_{tf} and c for M and associated value of ε'_{cm} from the FEM analysis. The result is compared with that by FEM in **Fig.11**. Both show that the applied moment increases with increasing crack length, and at around c/h=0.9, the maximum moment is attained, after which the moment decreases. The estimation by Eqs.(1), (2) and (3) shows good agreement near the peak load. Therefore, it can be concluded that the proposed estimation method is reasonable.

In order to estimate the sectional capacity of the lining from Eqs.(1), (2) and (3), two input parameters are necessary. The first parameter is the tensile strength carried by fibers f_{tf} which is the constant fiber stress assumed for the critical section at the peak load. The second parameter is the critical crack length c_{cr} which is the crack length of the critical section at the peak load. Knowing these two parameters and the applied compressive force, we can calculate the moment capacity by employing Eqs.(1), (2) and (3).

It is noticed from **Fig.8** that the transmitted tensile stress distribution does not change much with respect to the thickness of the lining. Therefore, the tensile strength carried by fibers f_{tf} to be used in the prediction of the sectional capacity is proposed to be determined from a test of a small specimen.

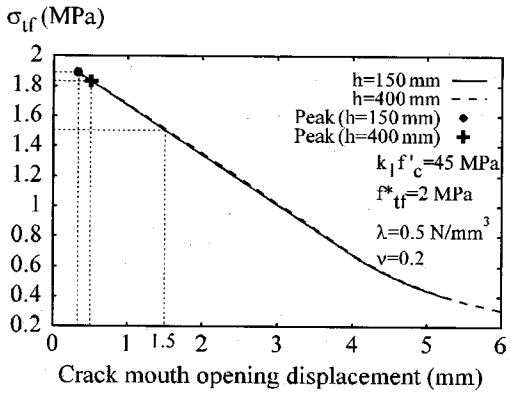

Fig.12 Approximation of f_{tf} from a small specimen.

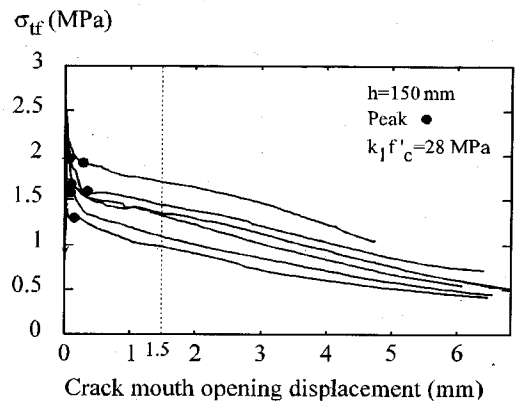

Fig.13 σ_{tf} computed from experimental results.

However, the transmitted tensile stress distribution changes with respect to the magnitude to the applied compressive force. Therefore, the effect of the compressive force on the transmitted tensile stress should be taken into account in the design procedure.

The second parameter, the critical crack length c_{cr}, is found to be dependent on the specimen size, the slope of the tension-softening curve and the magnitude of the applied axial compressive force as observed in **Fig.7**, **Fig.9** and **Fig.10**. Among these three affecting parameters, the slope of the tension-softening curve represents the fiber property and quality of the steel-fiber-reinforced concrete. The dependence of the critical crack length on the fiber property is not considered in the existing design. It should be taken into account for the quality control of the fibers. The slope of the tension-softening curve must therefore be estimated to obtain the appropriate critical crack length.

It is important to note that, in the estimation of the sectional capacity, the top compressive strain ε'_{cm} must not be greater than the ultimate compressive strain ε'_{cu} (see **Fig.3**). When the maximum compressive strain reaches the ultimate compressive strain, the failure mode is understood to change into the compressive failure. In any case, if the selected critical crack length gives the top compressive strain higher than the ultimate compressive strain, instead of being an input parameter, the critical crack length will be determined in such a way that the top compressive strain is equal to the ultimate compressive strain.

(2) Methods to determine the tensile strength carried by fiber and the critical crack length

As it is discussed in the previous section, in order to estimate the sectional capacity, the tensile strength carried by fibers f_{tf} and the critical crack length c_{cr} are necessary. In this section, a method to obtain the tensile strength carried by fibers f_{tf} from an experiment of a small beam is proposed. After that, a method to estimate the slope of the tension-softening curve from the same bending test is presented. The slope of the tension-softening curve is subsequently used for the determination of the appropriate critical crack length c_{cr}.

Considering Eqs.(1), (2) and (3), we know that for given values of ε'_{cm}, N′ and M, one can calculate the tensile stress carried by fibers σ_{tf} and the crack length c. In a bending test, if the top compressive strain ε'_{cm} is measured for the corresponding applied moment M, the tensile stress carried by fibers σ_{tf} and the crack length c can then be computed. Here, we use the result obtained from FEM analysis to investigate the method. From the applied moment M and the corresponding top compressive strain ε'_{cm} from FEM analysis, the tensile stress carried by fibers σ_{tf} is calculated and plotted with respect to the crack mouth opening displacement in **Fig.12** for the 150 mm and 400 mm specimens. Note that it is a pure bending case; therefore, there is no applied axial compressive force.

From the figure, it is noticed that σ_{tf} decreases when the crack mouth opening displacement increases, and σ_{tf} for both cases is almost the same for the same crack mouth opening displacement. From the experiments of small beams, it is difficult to identify the peak loads to be used for the determination of the tensile strength carried by fibers f_{tf} because load-displacement curves obtained in actual tests usually scatter a lot. Thus, instead of the peak, σ_{tf} at a specific crack mouth opening displacement will be used as the tensile strength

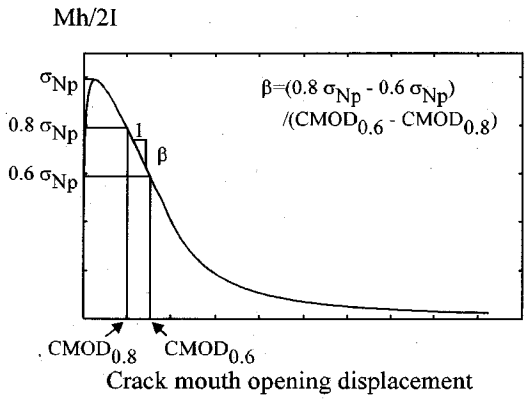

Fig.14 Definition of β.

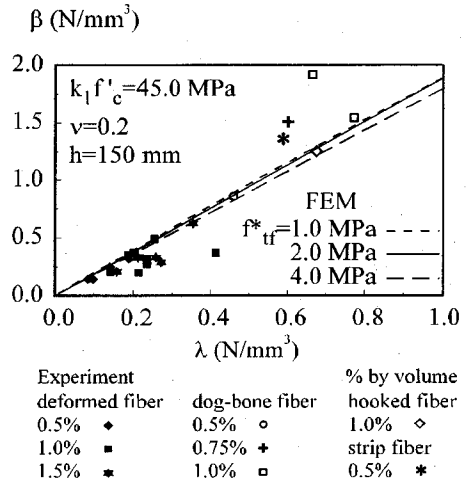

Fig.15 Relationship between β and λ.

carried by fibers f_{tf}. It is found in experiments that the crack mouth opening displacement at the peak load scatters but is always less than 1.5 mm for SFRC. This fact is noticeable in **Fig.13** which shows σ_{tf} computed from the applied moment M and the corresponding top compressive strain ε'_{cm} from experiments. Because σ_{tf} decreases when the crack mouth opening displacement increases, it is safe to use 1.5 mm as a reference. The rate of reduction of σ_{tf} with increasing crack mouth opening displacement is larger when the tension-softening curve is steeper, i.e., fiber bridging is of less quality. Therefore, this method assures the quality of fiber bridging, since f_{tf} is very small for poor fiber bridging. Using the small f_{tf} will subsequently necessitate using larger design sections. It is important to note that sections with the applied axial compressive forces are supposed to have smaller σ_{tf} at the peak loads than sections without the axial compressive force. Thus using σ_{tf} smaller than the value at the peak load of the section without the axial compressive force as f_{tf} also takes care of the reduction of f_{tf} for cases with the applied axial compressive force.

The practical method to measure ε'_{cm} and the experimental validation of this method are studied by Matsuoka et al.[10), 11)] To determine f_{tf}, one carries out a bending test on a small specimen and measures the axial strain at the top of the critical section when the crack mouth opening displacement is equal to 1.5 mm including the corresponding applied moment. From ε'_{cm} and M, f_{tf} is calculated from Eqs.(1), (2) and (3). This f_{tf} will be used in the prediction of the sectional capacity of the real sections. In the existing design provision, f_{tf} is also recommended to be determined from a bending test. With the maximum moment obtained from the test and the assumption that the maximum crack length is equal to 70% of the thickness, f_{tf} is calculated. However, it is observed that the critical crack length for SFRC members is usually longer than 70% of the thickness. Hence, limiting the crack length to 70% of the thickness inevitably leads to an overestimation of f_{tf}.

Next, a method to estimate the slope of the tension-softening curve is proposed. It is well-known that it is not practical to obtain the tension-softening curve directly from a direct tension test because the test is difficult and requires a sophisticated testing machine. In the present study, a method to estimate the slope of the tension-softening curve from a bending test is proposed.

It is noticed that the post-peak slope of the load-crack mouth opening displacement curve in the bending test is usually almost linear. Further more, it is also found that the slope has a unique relationship with the slope of the tension-softening curve. Because of its linearity, it is reasonable to define the post-peak slope of the moment-crack mouth opening displacement curve β as

$$\beta = \frac{0.8\sigma_{Np} - 0.6\sigma_{Np}}{CMOD_{0.6} - CMOD_{0.8}} \qquad (4)$$

where σ_{Np} is the normalized peak moment or the flexural strength, $CMOD_{0.6}$ and $CMOD_{0.8}$ are the crack mouth opening displacements when the applied loads are equal to 60% and 80% of the flexural strength, respectively (see **Fig.14**).

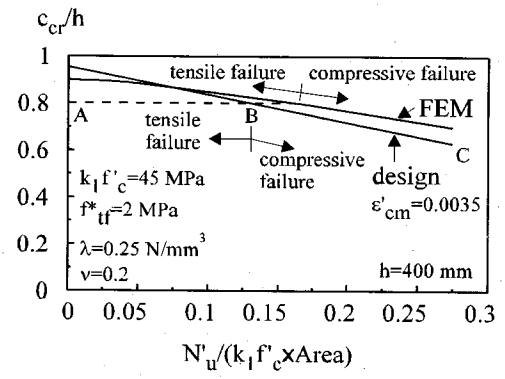

Fig.16 Design critical crack length.

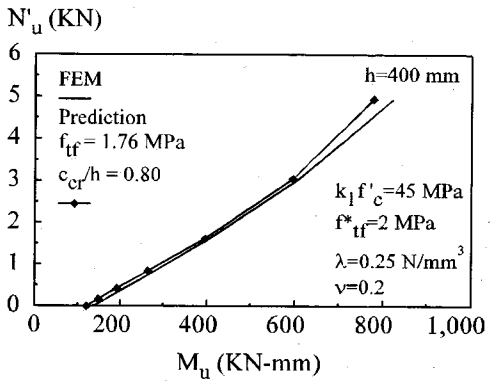

Fig.17 Interaction diagram with λ=0.25 N/mm^3.

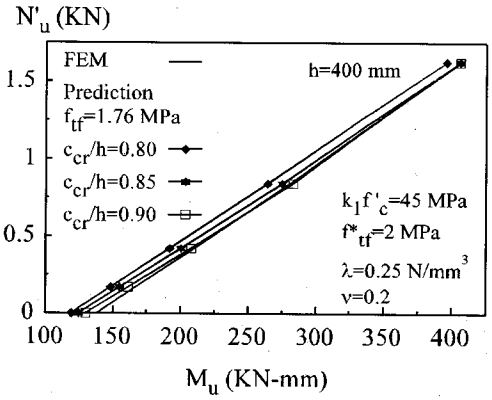

Fig.18 Prediction with different critical crack lengths.

Fig.15 shows the relationship between the post-peak slope of the normalized moment-crack mouth opening displacement β obtained from FEM analysis and the slope of the tension-softening curve λ defined in **Fig.6** for the specimen of 150 mm height with indicated values of f^*_{tf}. It is seen that the curve does not depend on the magnitude of f^*_{tf}. Experimental results by Matsuoka et al.[10), 11)] are also plotted in the same figure. FEM results fairly agree with experimental results.

From an experimental result of a bending test, the post-peak slope of the normalized moment-crack mouth opening displacement curve β is obtained. Then the slope of the tension-softening curve λ is estimated from the relationship between β and λ. The appropriate critical crack length to be used in the prediction of the sectional capacity is determined with the estimated λ.

Because the estimated bending moment capacity is larger with longer crack length, the selected critical crack length for each set of the lining thickness and the slope of the tension-softening curve must be shorter than the real crack length to ensure the safety in the design. However, it is practically impossible to get the real crack length. In this study, the critical crack lengths for different slopes of the tension-softening curves and different thickness are determined by FEM analysis. In the determination of the critical crack length, the fact that the critical crack length becomes shorter when the applied axial compressive force is larger must also be considered. **Fig.16** shows variation of the critical crack length with respect to the applied axial compressive force from FEM analysis of a specimen of 400 mm height. The figure also shows the crack length obtained from the design stress distribution when the top compressive strain ε'_{cm} is forced to be equal to the ultimate compressive strain ε'_{cu}. In the figure, the crack length A corresponds to the critical crack length at which the failure mode changes from the tensile failure to the compressive failure in FEM analysis. Note that, in the tensile failure, the top compressive strain ε'_{cm} at the peak load is less than the ultimate compressive strain ε'_{cu}. In this study, the crack length when the failure mode in FEM analysis changes from the tensile failure to the compressive failure will be selected as a critical crack length to be used in the prediction of the sectional capacity under the tensile failure mode because it is the shortest critical crack length under this failure mode. When the applied axial compressive force is higher than the one at point B in the figure, the failure mode of the section from the design stress distribution changes from the tensile failure to the compressive failure. Beyond point B, if the crack length A is still used in the prediction, it will result in the top compressive

Table 1 Design normalized critical crack length c_{cr}/h.

	h=200 mm	300 mm	400 mm
$0 \le \beta \le 0.46$	0.84	0.82	0.80
$0.46 < \beta \le 0.92$	0.80	0.77	0.73
$0.92 < \beta \le 1.85$	0.74	0.68	0.66

strain ε'_{cm} higher than the ultimate compressive strain ε'_{cu}. Thus, After the point B, the critical crack length must follow line BC which is the solution when the top compressive strain ε'_{cm} is equal to the ultimate compressive strain ε'_{cu}. As a conclusion, the critical crack length represents by lines ABC will be used in the design prediction. The proposed critical crack length is always shorter than the one from FEM analysis; thus, the prediction on the safe side is expected.

Fig.17 shows an interaction diagram of the moment and axial compressive force capacities of the section with the height of 400 mm by the proposed design method. The material properties are the same as in **Fig.16**. The tensile strength carried by fiber f_{tf} is obtained by the design method with the FEM result of the 150 mm specimen. The critical crack length obtained from the proposed method in **Fig.16** is used in the prediction. The prediction is compared with the result obtained from FEM analysis. From the comparison, a close and safe prediction is observed.

Fig.18 shows the interaction diagrams of the same problem with indicated values of the crack length. It is seen that if the critical crack length longer than the proposed critical crack length is used, the closer prediction may be obtained. However, the safe prediction cannot be guaranteed as the applied axial force becomes greater because the selected critical crack length may become longer than the real crack length.

Employing the same philosophy, we can determine the critical crack length for other sets of β (or λ) and h. In the design provision, a table will be prepared for designers to select the critical crack length according to given post-peak slope of the normalized moment-crack mouth opening displacement β and the lining thickness h. The post-peak slope of the normalized moment-crack mouth opening displacement β can be used in the table instead of the slope of the tension-softening curve λ because these two parameters almost have one to one relationship as shown in **Fig.15**. In this study, the relationship between β and λ in **Fig.15** is approximated as

$$\beta = 1.85\lambda. \qquad (5)$$

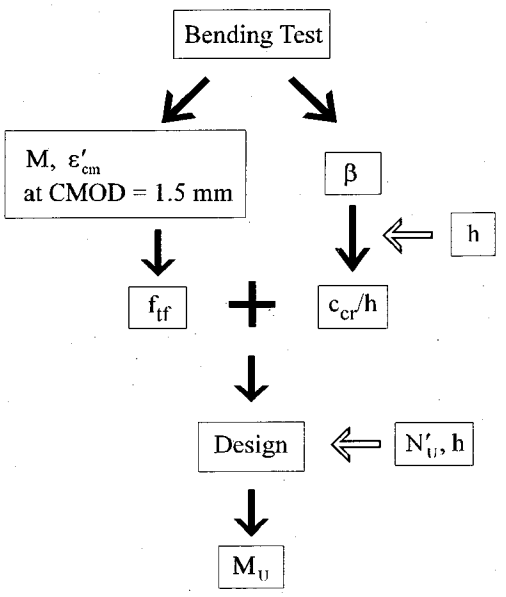

Fig.19 Flow of the proposed design method.

The critical lengths given in the design provision will correspond to the critical crack lengths for the tensile failure mode (line AB in **Fig.16**). The critical crack lengths under the compressive failure will be automatically obtained from Eqs.(1), (2) and (3) with the additional condition that the top compressive strain is equal to the ultimate compressive strain (line BC in **Fig.16**). **Table 1** shows an example table of the normalized critical crack length for linings with different thickness and β.

In this new design method, one obtain f_{tf} and β from a bending test of a small beam. From the obtained β and the thickness of the lining, an appropriate critical crack length will be selected from a provided table in the design provision. Using this critical crack length and f_{tf}, the sectional capacity can finally be calculated for any given applied compressive force from Eqs.(1), (2) and (3). In all cases, the top compressive strain must not be greater than the ultimate compressive strain ε'_{cu}. If the critical crack length from the design table leads to the top compressive strain higher than the ultimate compressive strain, the capacity of the section will be recalculated using the condition that the top compressive strain is equal to the ultimate compressive strain. In this case, the critical crack length from the table is not used in the prediction, and the crack length becomes one of the unknowns in the system of the equations (see **Fig.16**). The flow of the proposed design method is shown in **Fig.19**.

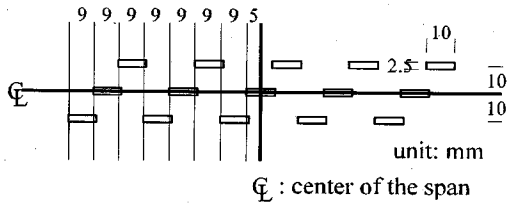

Fig.20 Position of strain gauges on the top of the beam.

Table 2 Tensile strengths carried by fibers from experiments.

Specimen No.	Mh/2I at CMOD=1.5 mm (MPa)	ε'_{cm} at CMOD=1.5 mm	f_{tf} (MPa)
1	2.85	0.0021	0.98
2	3.14	0.0019	1.09
3	3.77	0.0018	1.33
4	3.83	0.0016	1.35
5	4.11	0.0024	1.44
6	4.78	0.0021	1.70

6. EXPERIMENTAL INVESTIGATION

In this section, the proposed design method is examined with experimental results. The design method is employed in the prediction of the sectional capacity of big specimens by using the test results of small specimens. First, the four-point bending tests of small beams are performed. The cross-section of the beam is 150x150 mm, and the span length is 450 mm. Two point loads are symmetrically applied at 75 mm away from the center of the span. The material used is the steel-fiber-reinforced concrete with 1% by volume of straight deformed steel fibers. The compressive strength of the concrete is approximately equal to 33 MPa. In the test, a number of strain gauges are attached to the top of the beam at the center part of the span to measure the strain during loading as shown in **Fig.20**. The dimension of the strain gauges used is 2.5x10.0 mm. Many strain gauges have to be used because the crack path may be slightly different from the center alignment. A notch with the length of 10 mm is cut at the middle of the beam, and a clip gauge is attached to measure the crack opening displacement (see Matsuoka et al.[10), 11)]).

Fig.21 shows the experimental load-crack mouth opening displacement curves obtained from six beam specimens. It can be easily noticed that the load-crack mouth opening displacement curves scatter a lot. Especially, it is important to note that the load-carrying capacities differ very much from specimen to specimen even though the material is the same for all cases. Nevertheless, the post-peak slopes of all the curves show less difference.

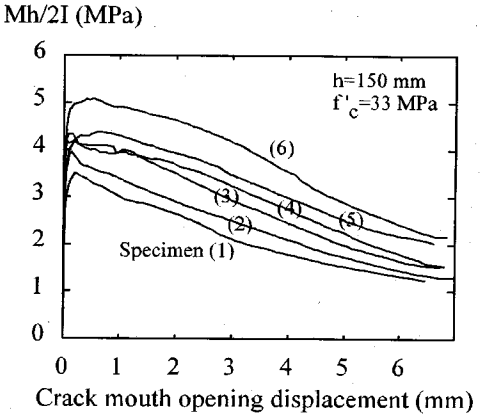

Fig.21 Experimental load-crack mouth opening displacement curves.

Table 3 β from the experiments.

Specimen No.	β (N/mm^3)
1	0.49
2	0.42
3	0.52
4	0.52
5	0.49
6	0.69

First, the tensile strength carried by fibers is determined. From **Fig.21**, the moment at the crack mouth opening displacement equal to 1.5 mm for each case is obtained. From the measurement data obtained from the strain gauges, axial compressive strain at the top of the critical section is determined at the same magnitude of the crack mouth opening displacement. From these two measured data, the tensile strength carried by fibers f_{tf} is computed by employing Eqs.(1), (2) and (3). The result is shown in **Table 2**.

Next, to be able to select the critical crack length provided in **Table 1**, the post-peak slope of the load-crack mouth opening displacement β must be determined from **Fig.21**. The obtained result is shown in **Table 3**.

The obtained f_{tf} and β will be used to predict the sectional capacity of a section with the height of 400 mm. The prediction result will be compared with experimental results. The material properties of the 400 mm section are of course the same as the 150 mm section. It is noticed from **Table 2** and **Table 3**

that the tensile strengths carried by fibers f_{tf} scatter a lot while the post-peak slopes of the load-crack mouth opening displacement curves β do not. Considering this fact, we will use the mean value of β to select the critical crack length from **Table 1**. From **Table 3**, it is found that the mean value of β is equal to 0.52 N/mm^3. Therefore, the normalized critical crack length equal to 0.73 will be used in the prediction.

It is not easy to find the appropriate f_{tf} to be used in the prediction from the obtained f_{tf} in **Table 2** due to the scattering. If the averaged value is used, it may result in the overestimation if the strength of the material in the real section is weaker than the averaged property. Furthermore, it is also known that bigger specimens may tend to have the weakest parts of the specimens that are weaker than the weakest parts of the smaller specimens. This is an additional size effect which results in the additional small reduction of the load-carrying capacity in bigger specimens. In this paper, various values of f_{tf} are tried as shown in **Fig.22**.

In **Fig.22**, f_{tf} equal the average $\bar{x}$ of the values in **Table 2**, the average minus one times standard deviation $\bar{x}-\sigma$, and the average minus two times standard deviation $\bar{x}-2\sigma$ are used ($\bar{x}$=1.32 MPa, σ=0.23 MPa from **Table 2**). It is found that the values of f_{tf} less than the average by one or more times standard deviation give safe predictions, compared with the experimental results. Note that the minimum value of f_{tf} in the six samples is equal to $\bar{x}-1.43\sigma$. In the same figure, it is also shown that if the tensile strength is neglected and the critical crack length is assumed to be equal to 50% of the thickness of the section, very low capacity is obtained which is the case of plain concrete. It then becomes clear that omission of the tensile resistance in the steel-fiber-reinforced concrete is very uneconomical.

In this paper, only six experimental data are used in the calculation of the tensile strength carried by fibers f_{tf}. To specify in the design provision the number of test specimens necessary for the determination of f_{tf}, and the way to determine f_{tf} from the results of many test data, statistical investigation on more experiments is necessary. This investigation is given by Matsuoka et al.[10),11)]

7. CONCLUSION

In the design of concrete tunnel linings, one of the limit states is the failure of a section after initiation and propagation of a crack. An increase in maximum resultant forces and greater toughness after the peak

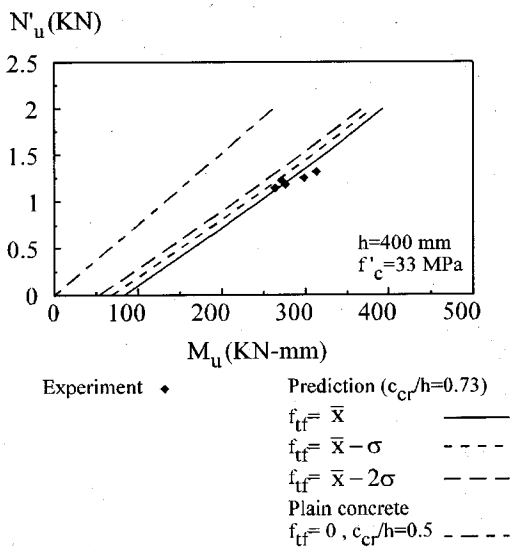

Fig.22 Prediction of the 400 mm specimen.

load are expected in linings with SFRC, due to the stress transmission across crack surfaces by fibers. To reflect such benefits of steel fibers in design, the design provision must take this stress transmission into account. The knowledge of fracture mechanics must be applied since the limit state is governed by the growth of a crack and the stress transmission across it.

The existing design provision[1)] for the evaluation of the sectional capacity of linings is based on fracture mechanics. In this design provision, a crack and the stress transmission across the crack are considered. Two major assumptions in the provision are that the transmitted stress is constant along the crack, and the maximum crack length is shorter than 70% of the thickness. From the result of the investigation in this study, it is found that the assumption of the constant transmitted stress is valid. It is also observed that the critical crack lengths in most cases are longer than 70% of the thickness. Therefore, the assumption of the maximum crack length equal to 70% of the thickness in the evaluation of the sectional capacity is to some extent acceptable since it is on the safe side. However, if the same assumption is employed in the determination of the tensile strength carried by fibers, it results in an overestimation. In fact, the critical crack length is found to be dependent on the thickness of the lining, the slope of the tension-softening curve and the magnitude of the applied axial compressive force. The slope of the tension-softening curve represents

the fiber property and quality of the steel-fiber-reinforced concrete. The dependence of the critical crack length on the fiber property should be taken into account for the quality control of the fibers.

In the modified design method proposed in this paper, the constant transmitted stress assumed along the crack and the crack length, both of which are necessary for the prediction of the sectional capacity, are proposed to be determined from the bending test of a small specimen. Methods to determine the two parameters requires only a load-crack mouth opening displacement curve and the information on the top compressive strain from the bending test. The prediction obtained from the new design method is numerically found to be safe and economical.

The method is also tested with the experimental data. It is observed that the load-crack mouth opening displacement curves obtained from experiments scatter a lot. Thus, to specify in the design provision the number of test specimens necessary and the way to determine the necessary parameters from the results of many test data, statistical investigation on more experiments is necessary. However, with the limited experimental data used in the study, the good prediction is observed. It is also shown that if the tensile resistance in SFRC is neglected, the uneconomical prediction will be obtained.

REFERENCES

1) Japan Railway Construction Public Corporation: *Recommendation for Design and Construction of Extruded Concrete Lining Method*, Yoshii Shoten, Tokyo, 1992 (in Japanese).
2) Dugdale, D.S.: Yielding of steel plates containing slits, *Journal of Mechanics and Physics*, Vol.8, pp.100-108, 1960.
3) Barenblatt, G.I.: The mathematical theory of equilibrium of cracks in brittle fracture, *Advances in Applied Mechanics*, Vol.7, pp.55-129, 1962.
4) Hillerborg, A.E., Modeer, M. and Petersson, P.E.: Analysis of crack formation and crack growth in concrete by means of fracture mechanics and finite elements, *Cement and Concrete Research*, Vol.6, pp.773-782, 1976.
5) Nirmalendran, S. and Horii, H.: Analytical modeling of microcracking and bridging in the fracture of quasi-brittle materials, *J. Mech. Phys. Solids*, Vol.40, No.4, pp.863-886, 1992.
6) Horii, H. and Nanakorn, P: Fracture mechanics based design of SFRC tunnel lining, *Size Effect in Concrete Structures*, Mihashi, H., Okamura, H. and Bazant, Z.P. eds., E&FN Spon, London, pp.429-440, 1993.
7) Nanakorn, P. and Horii, H.: A finite element with embedded displacement discontinuity, *Building for the 21th Century*, Loo, Y.C. ed., Vol.1, Giffith University (Gold Coast Campus), Australia, pp.33-38, 1995.
8) Nanakorn, P. and Horii, H.: Back analysis of tension-softening relationship, submitted to *Proceedings of JSCE*.
9) Nanakorn, P.: *Fracture Mechanics Based Design Method of SFRC Tunnel Lining*, Doctoral Dissertation, The University of Tokyo, Japan.
10) Matsuoka, S., Matsuo, S., Masuda, A. and Yanagi, H.: A test method for tensile property of steel-fiber-reinforced concrete, to be submitted to *Proceedings of JSCE*.
11) Matsuoka, S., Masuda, A., Matsuo, S. and Yanagi, H.: Verification of a fracture mechanics-based method to evaluate cross-sectional capacity of SFRC members, to be submitted to *Proceedings of JSCE*.

(Received July 17, 1995)

破壊力学に基づく鋼繊維補強コンクリートトンネルライニングの設計法

Pruettha NANAKORN・堀井秀之・松岡茂

本論文は破壊力学に基づく鋼繊維補強コンクリートトンネルライニングの断面耐力算定法を提案するものである．1992 年に制定された設計基準における破壊力学に基づく設計法の妥当性を検証し，その改良点を示した．さらに，不連続面を有する有限要素を用いた解析法による解析結果と実験結果に基づき，引張に関する材料特性値とその試験法，及び断面耐力の算定法を提案した．提案した方法に従い，高さ 15cm の梁の曲げ試験結果より材料の特性値を求め，算定された断面耐力と軸力と曲げを受ける高さ 40cm の梁の試験結果とを比較することにより提案する設計法の妥当性を検討した．

米国ITASCA（イタスカ）社開発の岩盤・地盤解析プログラム

未来設計企業 CRC

UDEC 3DEC 個別要素法(DEM)プログラム

個別要素法（離散要素法）は、1971年にDr.P.Cundallが発表した不連続体数値解析手法であり、岩盤や地盤をブロックや土粒子の要素の集合体と考え、個々の要素が隣接要素から受ける力により運動方程式にもとづき挙動する様子を時間差分式にて時刻繰返し計算する手法です。個別要素法は不連続力学の中心手法として位置づけられ、岩盤・地盤の崩落や安定性の解析、大深度地下空間、核廃棄物地下処理、鉱物資源開発等のプロジェクトおよび粒状体力学（粉体工学）の分野で有力な解析手段となっています。現在UDEC，3DECは全世界の研究機関・企業で標準コードとして広く使用されています。

オプション

■Barton-Bandisモデル

適用分野

- ●粒状物質の挙動解析
- ●鉱山採掘等　掘削解析
- ●地震応答解析
- ●ジョイント内流れ解析
  （浸透連成：UDEC）
- ●核廃棄物の熱応力解析
  （熱連成：UDEC）

■販売条件

UDEC・3DEC・FLAC

- ◆EWS（SUN-SPARC）
- ◆IBM-PC/AT及び互換機
- ◆UDECはソースコードで提供します。
- ◆3DEC・FLACはロードモジュールで提供します。

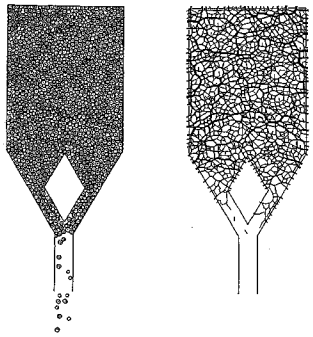

ホッパー内粒状体挙動解析

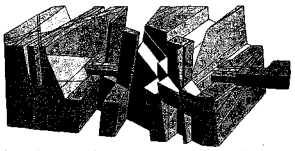

亀裂性岩盤の3次元掘削解析

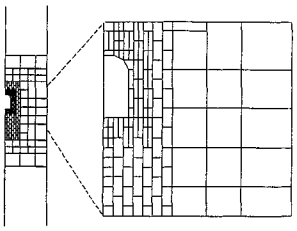

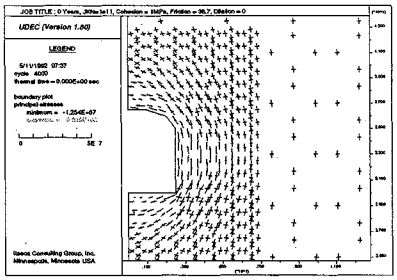

核廃棄物地中処理影響解析

FLAC 有限差分法(FDM)プログラム

FLACは個別要素法コードUDEC，3DECを発表したDr.P.Cundallが同様の有限差分ロジックを用いて連続体の塑性大変形の解析するために開発したコードで、現在、全世界で数多く使用されています。有限差分法は、地盤、岩盤を有限な領域内で離散化し、連動方程式と構成則を差分方程式として解析するもので、有限要素法に比べ非線形大歪が扱えることで大きな優位性を持っています。
FLACは小一大歪　非線形、動的一静動挙動を始めとし、豊富な機能　オプションを備えたPC、ワークステーション用の地盤解析コードです。

オプション

- ■ダイナミック解析モデル
- ■クリープ解析モデル
- ■熱解析モデル

適用分野

- ●斜面・盛土の設計、安定解析
- ●浅／深基礎設計
- ●アースダム、コンクリートダムの設計
- ●トンネルの設計
- ●核廃棄物貯蔵解析
- ●液状化解析

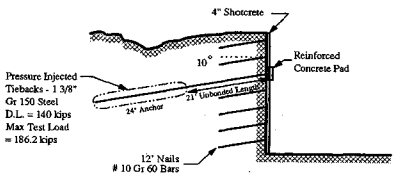

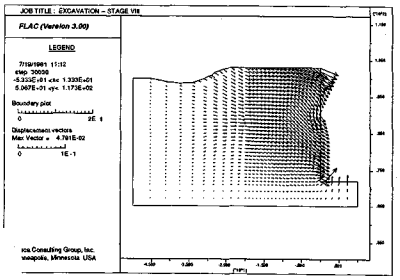

土　日本技術開発株資料室

株式会社CRC総合研究所

〒541
大阪市中央区久太郎町4丁目1-3
(06)241-4121　営業担当:岩　崎

土木学会論文集

昭和三十七年五月二十八日 第三種郵便物認可
平成八年二月十五日印刷
平成八年二月二十日発行
土木学会論文集（毎月二回二十日・二十一日発行）

定価二，五〇〇円（本体価格二，四五六円）